1st International Symposium on Laser Ultrasonics: Science, Technology and Applications
July 16-18 2008, Montreal, Canada

Impact of Magnetic Impurities on Transient Propagation of Coherent Acoustic Phonons in II-VI Ternary Semiconductors

Allen S. CROSS [1], Andrzej MYCIELSKI [2], Roman SOBOLEWSKI [1]

[1]Department of Electrical and Computer Engineering and the Laboratory for Laser Energetics, University of Rochester, Rochester, NY 14627-0231, USA
Phone: +1 585 275 1808, Fax: +1 585 273 1014; e-mail: acro@lle.rochester.edu, rsob@lle.rochester.edu
[2]Institute of Physics, Polish Academy of Sciences
PL-02668 Warszawa, Poland; e-mail: mycie@ifpan.edu.pl

Abstract
We detail our studies on the transient propagation of coherent acoustic phonons (CAPs) in Mn-doped $Cd_{1-x}Mn_xTe$ [(Cd,Mn)Te] diluted-magnetic and pure CdTe semiconductors. The CAPs were generated by femtosecond optical pulses and then time-resolved using one- and two-color pump-probe spectroscopy. Intrinsic lifetimes on the order of at least tens of nanoseconds of CAP oscillations were observed in (Cd,Mn)Te by pumping above and probing below the crystal bandgap. The CAP oscillation characteristics were well described by the propagating-strain model with the electronic stress as the excitation mechanism. Fitting the CAP frequency dependence on the probe wave vector while including the dispersion effect of the (Cd,Mn)Te refractive index, resulted in a very accurate determination of the crystal acoustic-phonon velocity and its increase with the Mn-doping increase, as well as the temperature-related changes of the acoustic velocity in pure CdTe single crystals.
Keywords: Laser ultrasound, coherent acoustic phonons, diluted magnetic semiconductors, femtosecond pump-probe spectroscopy

1. Introduction

The $Cd_{1-x}Mn_xTe$ [(Cd,Mn)Te] is a widely studied diluted-magnetic semiconductor (DMS), known for its many inherent properties, such as a widely tuneable bandgap ranging from 1.53 eV to 2.50 eV (near-infrared to visible range of optical radiation) and a stable zinc-blend structure for Mn concentrations up to $x \approx 0.70$. The highly researched topic of carrier and spin dynamics within (Cd,Mn)Te has lead to many potential applications, ranging from Faraday isolators to X-ray and γ-ray detectors [1]. In this paper, we present our research into unravelling the coherent phonon dynamics of the (Cd,Mn)Te system. Coherent acoustic phonons (CAPs) have been recently studied in other semiconductors such as GaN [2,3] and GaAs [4,5], as well as in various thin-films [6], and superlattices [7]. Possible applications of long-lived CAPs include ultrasonic imaging [3] and high frequency acoustic-optic modulation [5].

We use both single- and two-color pump-probe spectroscopy to perform systematic measurements on determining the phonon dynamics in the DMS (Cd,Mn)Te for several Mn concentrations. Our setup allows room temperature probing from just above the energy gap E_g to 0.3 – 0.4 eV below E_g. A cryostat was also employed for temperature dependent CAP measurements.

2. Fabrication and experimental methods

The single-crystal samples were fabricated using a modified vertical Bridgman method in which a seed crystal of CdTe was placed in an ampoule with a melt of Cd, Te and Mn. Because the segregation coefficient of Mn in (Cd,Mn)Te is near unity, the crystal is considered highly homogeneous. After crystallization, the sample was annealed in Cd to fill the Cd vacancies, thereby further improving uniformity and increasing resistivity [1]. Crystals of ~0.7-mm-width with x = 0.01, 0.05, and 0.09 were fabricated as well as pure CdTe. The samples were subsequently polished on the front and back surfaces.

The optical pump and probe beams were generated using a Ti:Sapphire laser with a 76 MHz repetition rate and a 100-fs-wide pulse output tuneable from 720 to 950 nm (1.71 eV to 1.30 eV). The pump pulse had a fluence of ~0.4 μJ/cm^2/pulse, travelled through an acousto-optic modulator operating at 243 kHz, and was focused at a normal incidence to the plane of the crystal. The probe pulse, at a 45° incidence to the crystal plane, had a non-invasive fluence of ~0.016 μJ/cm^2/pulse. For the single-color spectroscopy, the pump and probe beams were crossed polarized and an analyzer was placed before the detector to block the scattered pump light. The probe reflection was collected by a 125-MHz photodetector whose output was fed to a lock-in amplifier tuned to 243 kHz modulation frequency.

For the two-color spectroscopy, the pump beam passed through a BBO crystal for second harmonic generation, and eventually was screened out by an optical filter before the photodetector. In this arrangement, the pump photon energy is high above the (Cd,Mn)Te E_g, while the probe beam tuned from just above to far below E_g. The latter allowed low attenuation and dispersion measurements, while maintaining efficient generation of CAPs. For low temperature measurements a helium-cooled, vacuum loading continuous flow cryostat was used.

3. Results

3.1. Theoretical approach

Electronic or thermal stress generated by the absorption of the 100-fs-wide pump pulse results in a propagating strain pulse orthogonal to the sample surface. Probe light reflects off of the strain pulse due to altered optical properties induced by the lattice mismatch. As the CAP pulse propagates further into the crystal, this reflection undergoes constructive and deconstructive interference with the independent surface reflection. The equation that describes the time evolution of normalized optical differential reflectivity ($\Delta R/R$) induced by the CAPs is:

$$\Delta R / R = A\sin(2\pi ft - \phi)\exp(-t / \tau_d), \quad (1)$$

where A is the pump-photon energy dependent amplitude, f is the CAP frequency, and φ is the phase of the oscillations. The experimental decay rate of the oscillations τ_d is a combination of the intrinsic phonon decay time τ_{phonon} and the probe light penetration depth ς, and is given by

$$\frac{1}{\tau_d} = \frac{1}{\tau_{phonon}} + \frac{1}{\varsigma / v_s}, \quad \text{.....(2)}$$

where v_s is the velocity of sound of the (Cd,Mn)Te crystal.
Since the oscillations are governed by the optical self-interference of the probe light reflected from the sample surface and propagating strain pulse, the equation modeling the oscillation frequency is [8]:

$$f = \frac{2n(\lambda)v_s}{\lambda_{probe}} \cos(\theta) = \frac{n(\lambda)v_s}{\pi} k_{probe} \cos(\theta), \quad \text{.....(3)}$$

where λ_{probe} and k_{probe} are the wavelength and wave number of the probe, respectively, n is the index of refraction, and θ is the incident angle of the probe beam to the normal of the sample surface.

3.2. Experimental results and discussion

3.2.1. CAP pulse detection

To analyze the CAPs, the experimental pump-probe response (fig. 1 inset) was first prepared by truncating the initial electronic contribution to $\Delta R/R$, and the subsequent subtraction of exponential electron-hole recombination decay. The result shown in fig. 1 is the CAP oscillation (dots) and can be very well fitted by eq. (1) (solid line fig. 1).

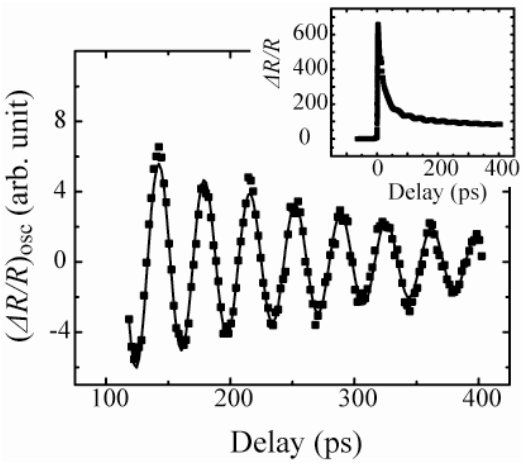

Figure 1. (■) CAP oscillation measured by the single-color pump probe spectroscopy in $Cd_{0.91}Mn_{0.09}Te$. Solid line is a numerical, damped sinusoidal fit. The inset shows the full experimental $\Delta R/R$ photoresponse.

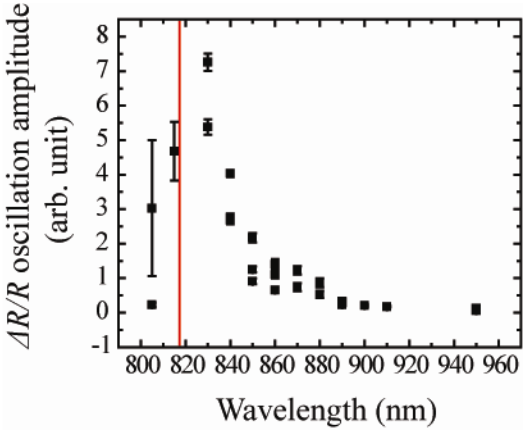

Figure 2. CAP oscillation amplitudes of CdTe measured using the two-color pump-probe spectroscopy. The red line indicates E_g of CdTe.

In two-color spectroscopy the strength of electronic stress induced CAP should be near constant for pump energies far above E_g [9]. Figure 2, however, shows that the oscillation amplitude peaks as the energy of probe photons approaches E_g.

3.2.2. CAP analysis in (Cd,Mn)Te

Figure 3 shows the dispersion curve, where we see that the slope of f with respect to k_{probe} is directly proportional to the $n(\lambda)v_s$ product. For $h\nu_{probe} << E_g$, n is a constant, however, for the E_g values of (Cd,Mn)Te with x from 0.00 to 0.09, we must use the $n(\lambda)$ form. For room-temperature measurements, we use the $n(\lambda)$ dispersion model for (Cd,Mn)Te described by Schubert *et al.* [10]:

$$n(\lambda)^2 = A + \frac{BE^2}{1-\left(E/C\right)^2} \text{ , for } E < C, \quad \text{.....(4)}$$

where A and C are x dependent parameters and B is a constant. For low-temperature measurements, however, we use the four oscillators Sellmeier's formula described by Hlídek *et al.* [11]:

$$n^2(\lambda) = a + \sum_{i=1}^{4} \frac{g(T)_i}{E(T)_i^2 - h\nu_{probe}^2}, \quad \text{.....(5)}$$

where a is a constant, and terms for i = 1 are contributions from the optical transition near E_g, terms for i = 2 and 3 are higher transitions, and the term i = 4 denotes lattice vibrations [11].

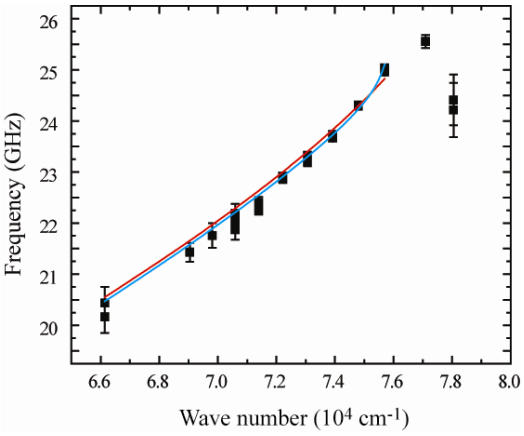

Figure 3. Dispersion curve for CdTe at room-temperature. (Red) Fitting using Schubert's equation for $n(x)$. (Blue) Fitting using Sellmeier's formula for $n(T)$.

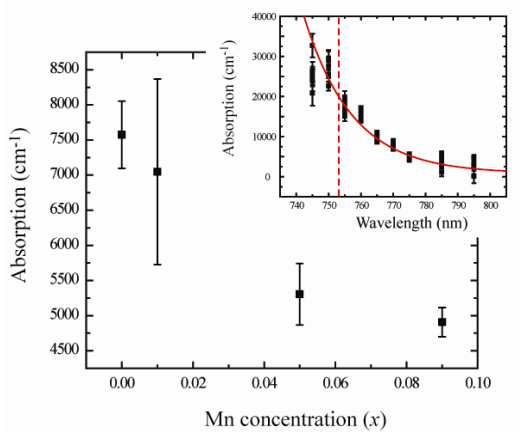

Figure 4. Absorption coefficient measured using single-color pump-probe spectroscopy at 0.97E_g for various Mn concentrations. The inset shows the wavelength dependence of α for x = 0.09. The red line an exponential fit serving as a guide to the eye. The dotted line indicates E_g = 1.65 eV (λ_g = 753 nm)..

Table 1. CAP measurements and $Cd_{1-x}Mn_xTe$ parameters for several x

Crystal	surface plane	$E_g(x)$ [eV]	λ_g [nm]	v_s [m/s]	α [cm^{-1}] (at 0.97 E_g)
CdTe	(111)	1.528	811	3578 ± 37	7574 ± 478
$Cd_{0.99}Mn_{0.01}Te$	(011)	1.541	805	3445 ± 7	7046 ± 1320
$Cd_{0.95}Mn_{0.05}Te$	unknown	1.594	778	3481 ± 18	5305 ± 437
$Cd_{0.91}Mn_{0.09}Te$	(111)	1.646	753	3593 ± 1	4907 ± 207

For our room-temperature measurements, we substituted Eq. (4) into Eq. (3) in order to obtain an accurate fit for v_s from our dispersion curves. A tabulation of our x dependent results is given in Table 1. Although no definitive conclusion regarding x dependence can be made from Table 1, we note that the fastest sound velocities are obtained in CdTe and $Cd_{0.91}Mn_{0.09}Te$, which were both cut along the (111) surface plane.

Using Eq. (2) and the fact that at the wavelengths near E_g, $\tau_{phonon} >> \varsigma/v_s$, we can determine α by a reduced relation of $1/\tau_d = \alpha v_s$. Figure 4 shows the inverse dependence of α on x, which warrants further investigation. The α values are given in Table 1, and were calculated at $h\nu_{probe} = 0.97E_g$, where we used $E_g = 1.528 + 1.316x$ [eV] [12]. The inset in Fig. 4 shows the λ dependence of α for CdTe measured using the single-color pump-probe spectroscopy. We note that CAP generation still occurs while pumping even well below the bandgap. This is indicative of both the dominant electronic stress (as opposed to thermal) in generation of CAPs and the existence of extended band-tail-states in (Cd,Mn)Te [13]. Furthermore, Wang *et al.* [13] calculated, the electronic-to-thermal stress ratio for $Cd_{0.91}Mn_{0.09}Te$, and found that for pump wavelengths near E_g, it was ~300.

Finally, we note that in our two-color measurements at long wavelengths, where $h\nu_{probe} << E_g$, α approached zero, which meant the oscillations did not show any measurable decay within the 400-ps-window of our spectroscopy setup. This lead to the conclusion that the τ_{phonon} value must in the nanosecond range.

3.2.3. Cryogenic analysis of CAPs in CdTe

In a similar manner as above, we substituted Eq. (5) into Eq. (3) to obtain a v_s fit for the temperature dependence. All cryogenic measurements were made using the two-color pump-probe method. Table 2 shows the results of the fitting where the $E_g(T)$ was calculated using the Manoogian-Wooley equation for CdTe given by Fonthal *et al.* [14]. Figure 3 shows fittings using both the Schubert (red line), and the Sellmeier (blue line) $n(\lambda)$ model. A comparison of both fittings shows a slight variation in v_s (~70 m/s or ~2%).

Table 2. Temperature measurements of CAPs in CdTe

Temperature (K)	E_g(T) [eV]	λ_g [nm]	v_s [m/s]
293.0 ± 0.1	1.516	818	3509 ± 3
200 ± 3	1.553	799	3519 ± 3
115 ± 4	1.583	783	3549 ± 12
26 ± 1	1.605	772	3572 ± 5

4. Conclusion

We presented our systematic research on the CAP dynamics within the ternary II-VI semiconductor (Cd,Mn)Te, using pump-probe spectroscopy as the means for generation and detection of CAPs. The measurements beget several interesting attributes such as CAP lifetimes of at least tens-of-nanoseconds, with a direct dependence on x.

Furthermore, the Schubert index model and the Sellmeier equation fit the dispersion curves precisely for both *x*- and *T*-relevant data, respectively. Using the methods of experimentation and analysis presented here, future measurements should help us to better describe phonon dynamics and establish a unified (Cd,Mn)Te $n(\lambda)$ model dependent on both temperature and Mn impurities.

Acknowledgements

This work was partially funded by the US NSF-NIRT grant ECS-0609140 (work in Rochester), and by the Polish Ministry of Science grant PBZ-KBN-044/PO3/2001 (work in Warsaw). A. S. C. acknowledges support from the Frank Horton Graduate Fellowship Program at the University of Rochester Laboratory for Laser Energetics, funded by DOE. The support of DOE does not constitute an endorsement by DOE of the views expressed in this article.

References

1. A. Mycielski *et al.*, 'Is the (Cd,Mn)Te crystal a prospective material for X-ray and γ-ray detectors?', *Phys. Stat. Sol*. (C), 2, pp 1578–1585, 2005.
2. S. Wu *et al.*, 'Time-resolved intervalley transitions in GaN single crystals', *J. Appl. Phys.*, 101, 043701, 2007.
3. K-H. Lin *et al.*, 'Two-dimensional nanoultrasonic imaging by using acoustic nanowaves', *Appl. Phys. Lett*., 89, 043106, 2006.
4. J. Miller *et al.*, 'Near-bandgap wavelength dependence of long-lived travelling coherent longitudinal acoustic phonons in GaSb-GaAs heterostructures', *Phys. Rev. B*, 74, 113313, 2006.
5. O. Matsuda *et al.*, 'Acoustic phonon generation and detection in GaAs/$Al_{0.3}$-$Ga_{0.7}$As quantum wells with picoseconds laser pulses', *Phys. Rev. B*, 71, 115330, 2005.
6. Y-K. Huang *et al.*, 'Generation of coherent acoustic phonons in strained GaN thin films', *Appl. Phys. Lett.*, 79, pp 3361-3363, 2001.
7. B. Glavin *et al.*, 'Generation of high-frequency coherent acoustic phonons in superlattices under hopping transport. I. Linear theory of phonon instability', *Phys. Rev. B*, 65, 085303, 2002.
8. C. Thomsen *et al.*, 'Surface generation and detection of phonons by picoseconds light pulses', *Phys. Rev. B*, 34, pp 4129-4137, 1986.
9. S. Wu *et al.*, 'Femtosecond optical generation and detection of coherent acoustic phonons in GaN single crystals', *Phys. Rev. B*, 76, 085210, 2007.
10. D. Schubert *et al.*, 'Composition and wavelength dependence of the refractive index in $Cd_{1-x}Mn_xTe$ epitaxial layers', *Appl. Phys. Lett.*, 60, pp 2192-2194, 1992.
11. P. Hlídek *et al.*, 'Refractive index of CdTe: Spectral and temperature dependence', *J. Appl. Phys.*, 90, pp 1672-1674, 2001.
12 J. Furdyna, 'Diluted magnetic semiconductors', *J. Appl. Phys.*, 64, pp R29-R64, 1988.
13. D. Wang *et al.*, 'Time-resolved dynamics of coherent acoustic phonons in Cd,MnTe diluted-magnetic single crystals', *Appl. Phys. Lett.*, 90, 211905, 2007.
14. G. Fonthal *et al.*, 'Temperature dependence of the band gap energy of crystalline CdTe', *Jour. Phys. Chem. Sol.*, 61, pp 579-583, 2000.